Journal of Alloys and Compounds

Flexible lead-free NBT-BT-PVDF composite films by hot pressing for low-energy harvesting and storage

--Manuscript Draft--

Manuscript Number:	JALCOM-D-21-04954
Article Type:	Full Length Article
Keywords:	composite materials; polymers; piezoelectricity; energy storage materials; Energy harvesting
Abstract:	The idea of this work is finding the way to efficiently and safely use mechanical energy released in small quantities around us to power up small-scale electronic devices used in everyday life. To this purpose, flexible lead-free piezoelectric composite films were prepared by hot pressing. Different amounts (30, 35 and 40 vol%) of lead-free piezoelectric material bismuth sodium titanate-barium titanate were implemented in the matrix of polyvinylidene fluoride under carefully optimized conditions of temperature and pressure, obtaining flexible films with quite homogeneous distribution of piezo-active filler. ATR-FTIR analysis revealed that hot pressing the flexible films caused a transformation of electro-inactive PVDF α-phase into electro-active β and γ phases. Dielectric measurements evidenced an increase of the permittivity with the active phase increasing. Anelastic measurements showed that the elastic modulus increases as well with the fraction of active ceramic phase. Flexible polymer-composites demonstrated notable properties both for energy storage and energy harvesting application.

Link to published version: https://dx.doi.org/10.1016/j.jallcom.2021.161071

Statement of the novelty

During presented investigation flexible composite films made of lead-free NBT-BT filler and PVDF matrix, especially NBT-BT-PVDF 30, have shown high potential to be used for efficient environmentally safe low-energy storage and harvesting devices.

Flexible lead-free NBT-BT-PVDF composite films by hot pressing for low-energy harvesting and storage

M. Vijatovic Petrovic[1], F. Cordero[2], E. Mercadelli[3], E. Brunengo[4], N. Ilic[1], C. Galassi[3], Z. Despotovic[5], J. Bobic[1], A. Dzunuzovic[1], P. Stagnaro[4], G. Canu[6], F. Craciun[2]

[1]Institute for multidisciplinary research, University of Belgrade, Kneza Viseslava 1, 11 000 Belgrade, Serbia

[2]CNR-ISM, Istituto di Struttura della Materia, Area della Ricerca di Tor Vergata, Via del Fosso del Cavaliere, 100, I-00133, Rome, Italy

[3]CNR-ISTEC, Istituto di Scienza e Tecnologia dei Materiali Ceramici, Via Granarolo 64, I-48018 Faenza, Italy

[4]CNR-SCITEC, Istituto di Scienze e Tecnologie Chimiche "Giulio Natta", Via de Marini 6, 16149, Genoa, Italy

[5] Institute Mihajlo Pupin, Volgina 15, 11000 Belgrade, Serbia

[6] CNR-ICMATE, Istituto di Chimica della Materia Condensata e di Tecnologie per l'Energia, Consiglio Nazionale delle Ricerche, Via de Marini 6, 16149, Genoa, Italy

Abstract

The idea of this work is finding the way to efficiently and safely use mechanical energy released in small quantities around us to power up small-scale electronic devices used in everyday life.

To this purpose, flexible lead-free piezoelectric composite films were prepared by hot pressing. Different amounts (30, 35 and 40 vol%) of lead-free piezoelectric material bismuth sodium titanate-barium titanate were implemented in the matrix of polyvinylidene fluoride under carefully optimized conditions of temperature and pressure, obtaining flexible films with quite homogeneous distribution of piezo-active filler. ATR-FTIR analysis revealed that hot pressing the flexible films caused a transformation of electro-inactive PVDF α-phase into electro-active β and γ phases. Dielectric measurements evidenced an increase of the permittivity with the active phase increasing. Anelastic measurements showed that the elastic modulus increases as well with the fraction of active ceramic phase. Flexible polymer-composites demonstrated notable properties both for energy storage and energy harvesting application.

Key words: composite materials, polymers, piezoelectricity, energy storage materials, energy harvesting

1. Introduction

An important task of the scientific community is to find the way of using the enormous amount of mechanical energy released through the vibrations in everyday life, *e.g.* by human walking, transportation movement, sound waves etc. as a renewable and safe energy source. The perspective of exploiting the mechanical energy of the surrounding environment can have a huge influence on our daily life. In this way, many of the health controlling devices, safety devices, sensors, alarms, lights and other small devices could be powered completely independently from external electricity sources (such as electricity grid and batteries), thus highly reducing our dependence from them as well as our total energy consumption. Piezoelectric generators have great potential for powering low-power portable devices and self-powered electronic systems by extraction of mechanical energy. The advantage of the piezoelectric mechanism over other conversion mechanisms lies in its high energy density and scalability across a wide range of sizes. Thus far piezoelectric generators commercially available are mostly lead-based materials. These materials based on lead-zirconate titanate (PZT) have shown the best piezoelectric performance in many commercial applications [1-11]. However, the family of lead-based materials is now facing the challenge due to its environmental incompatibility. The presence of lead, a toxic heavy metal, implies danger during the manufacture, use, and disposal of these materials. Most of all, recent global restrictions are demanding the removal of lead from all consumer items, which has stimulated urgent solicitation for lead-free substitutes that can have piezoelectric properties comparable to the ones obtained from the lead-containing materials [12]. During previous investigations, barium titanate (BT) and sodium bismuth titanate (NBT) based

materials synthesized in specific compositions, have shown to be among lead-free piezoelectrics with the highest d_{33} coefficients for possible replacement of PZT [2, 12-21]. Specifically, the NBT is a piezoelectric material with strong ferroelectricity and high remnant polarization at room temperature [13, 22-23]. The main obstacle to its application is that it possesses high coercive field and high conductivity preventing easy poling process necessary for good piezoelectric performance. In order to overcome this problem, different solid solutions have been developed during recent years [12-13, 17, 23]. Solid solution with barium titanate, (1-x) $[(Bi_{0.5}Na_{0.5})TiO_3]$-$x$$BaTiO_3$ have drawn significant attention due to the existence of a morphotropic phase boundary (MPB) region by simultaneous presence of rhombohedral and tetragonal phases for x about 0.06-0.07. [24-25]. It was detected that in this narrow MPB region (6-7% BT), NBT-BT exhibits enhanced performance. Besides high remnant polarization this ceramic is known for its high values of dielectric permittivity [23-26].

A recent challenge in electronics is also the utilization of flexible devices with the ability to bend into diverse shapes, which expands the applications of modern electronic devices in different areas. At the same time, polymer-based composites provide the advantages of being flexible, versatile, lightweight, low cost, and able to conform to complicated shapes, while typically involving low-temperature fabrication processes [2-7, 9-11,22]. Flexibility of electronic devices based on composites made of a lead-free piezo-active phase embedded in a polymer matrix will enable easy implementation in clothing, shoes and other accessories. Non-toxicity, impressive flexibility and biocompatibility make them a very good choice also for wearable electronics [27-29].

The polyvinylidene fluoride (PVDF) is the polymer matrix of choice for these applications. Flexible composites based on PVDF can be prepared by solvent casting, melt

blending and/or molding methods. Taking into account the relatively low melting temperature of this polymer (~180 ^{o}C), a smart way of flexible films preparation was here developed by designing a set up for hot pressing and preparation of flexible films based on PVDF polymer matrix. The hot pressing method was preferably used in order to avoid solvents that are usually used for PVDF dissolution, like dimethylformamide (DMF) [30-32]. This simple but rarely exploited concept of making flexible composites has attracted significant interest of science community since the process is facile and cost-effective. The PVDF polymer is a material with pretty complex molecular and crystalline structure and its properties are highly dependent on the heterogeneity of the system itself. It is indeed a semi-crystalline material with five polymorph crystalline phases that are defined by the conformation of the polymer chains [31, 33-34]. The most common crystalline phase is the non-polar α-phase made up of the combination of helical and zigzag conformations expressed by the trans-gauche-trans-gauche` conformation sequence (TGTG`). The trans-gauche conformation has an antiparallel packing motif in order to relax the interactions of fluorine atoms in neighbouring chains [33-34]. Since, this phase shows no polarity, it does not possess piezo- and pyroelectric properties, hence neither ferroelectric properties. The other polymorphs β, γ and δ are polar. In particular, the β-phase is made of all-trans conformations (TTTT) in which the carbon chains are aligned in a more straight mode (zigzag). The most preferable is the electroactive β-phase, which shows high polarity, high spontaneous polarization and piezoelectric coefficient (13-28 pC/N) [31-34]. The PVDF molecular interactions are governed by the short-range Van-der-Waals forces and hence low potential barriers for the rotation of chain molecules enable easy conversion between the polymorphs. Slightly more stable is the non-polar α-phase in comparison with the polar β-phase [33-35]. Literature data have already shown that the ferroelectrically inactive α-phase of PVDF

can be converted into electroactive phases β and/or γ by pressing, stretching at elevated temperatures, uniaxial tension, electrical poling, annealing, compression moulding etc. [31,34, 36-38]. This indicates the possibility of the co-existence of different polymer phases in the material at the same time which influence the electrical properties of the material as well as potential applications. Chu *et al.* also demonstrated that by combining non-polar and polar crystalline modifications of PVDF, very high energy density can be achieved, which is highly important for the energy storage application [39]. Moreover, inclusion of fillers in the polymer matrix and formation of polymer composites may enable the nucleation of electroactive β-phase. Some authors have shown that inclusion of barium titanate can make the β-phase to nucleate predominantly, but this process is highly dependent on the filler size [31, 35]. Others evidenced that addition of $NiFe_2O_4$ and $CoFe_2O_4$ in a certain percentage can guarantee the formation of 90% of β-phase. It was explained that CH_2 bonds of PVDF and negatively charged ferrites surface have strong interactions, which induce the formation of all trans conformation with consequent β- crystallographic phase stabilization [31]. There are studies where, along with the addition of the filler (*e.g.* barium titanate), stretching was performed in order to obtain mainly β-phase in the material [35].

This research was focused on the preparation of flexible composite films, by combining a highly flexible PVDF polymer matrix with lead-free piezoelectric perovskites, $0.94[(Bi_{0.5}Na_{0.5})TiO_3]$-$0.06BaTiO_3$ (NBT-BT), in different ratios. Since a rather limited number of papers dwelled with these particular composites, a crucial point of this investigation is to show that this material is quite versatile and possesses functional properties which are sensitive to both microscopic and chemical modifications. All the evidences reviewed above show that proper tailoring of material properties is possible by selecting adequate polymer and filler pairs, which

combined with the choice of a suitable processing method will allow the improvement of existing and the widening of the potential applications. Using a lead-free piezoelectric polymer-based composite material for low-energy harvesting and energy storage for always-on devices paves the way to a new type of safe production and usage of energy for everyday life.

2. Experimental

2.1. Preparation of active phase powders and flexible composite films

Powders of $0.94[(Bi_{0.5}Na_{0.5})TiO_3]$-$0.06BaTiO_3$ were synthesized by solid state route. The stoichiometric amounts of $BaCO_3$ (99.0%, Merck), TiO_2 (99.9%, Degussa), Na_2CO_3 (99.5%, Merck), Bi_2O_3 (99.9%, Aldrich) were ball milled in ethanol for 48 h. The dried precursors mixture was then sieved at 250 μm and calcined at 800°C for 1 h. The calcined NBT-BT powder was finally ball milled in ethanol for 120 h, dried and sieved at 250 μm. The preparation process has been optimized in order to achieve pure perovskite phase and good piezoelectric properties of the achieved ceramics.

Commercial PVDF powder (Alfa Aesar) and the previously synthesized NBT-BT powders were mixed in three different ratios: namely, 30, 35 and 40 vol% of NBT-BT powders. Samples were named according to the amount of filler as NBT-BT-PVDF30, NBT-BT-PVDF35 and NBT-BT-PVDF40, respectively. The powder of the active phase was mixed with PVDF powder. The samples have been further subjected to a hot-pressing process using a custom built set up. The hot pressing procedure consisted of heating up to 190 ^oC with applying a pressure of 5 MPa and then natural cooling.

2.2. Characterization of powders and composite films

The structures of synthesized NBT-BT powders and composite films were investigated using XRD (Bruker D8 Advance X-ray Diffractometer and Rigaku MiniFlex 600 instrument respectively) measurements. The particles were also morphologically characterized with a LEO 1450VP (LEO Electron Microscopy Ltd) SEM microscope. The morphology of the composites was investigated by a Tescan VEGA TS 5130MM microscope. Both the external surface and the transversal section (obtained by fracture of the samples) were observed. The flexible composites were studied by Infrared spectroscopy, which is a useful technique to identify the crystalline phases of the PVDF matrix and to estimate the amount of the electroactive phases (β and/or γ). The analyses were carried out in attenuated total reflectance (ATR) mode by PerkinElmer Spectrum Two™ FTIR spectrometer and collecting spectra in the 4000-400 cm^{-1} wavenumber range. Equation 1 was used to estimate the relative fraction of the electroactive phase(s) (F_{EA}) on normalized spectra, subtracted from the contribution of the filler [32, 40-41]:

$$F_{EA} = \frac{I_{EA}}{1.26\, I_{\alpha} + I_{EA}} * 100 \qquad (1)$$

where I_{EA} is the absorbance of the band at about 840 cm^{-1} that can be assigned to β and/or γ phase, I_{α} the absorbance of a characteristic band of the α phase and 1.26 the ratio between the absorption coefficients at the respective wavenumbers. As suggested by X. Cai *et al.*, [42] when β and γ phases were present simultaneously, the peak-to-valley height ratio between the two peaks around 1275 and 1234 cm^{-1} was used to separate the two contributions (F_{β}) and (F_{γ}). The composite materials as well as the neat PVDF were subjected to differential scanning calorimetry (DSC) in order to establish the crystallinity degree (X_C). Two repeats for each sample were performed with a Mettler DSC 821^e instrument, by heating from room temperature up to 220°C at a scan rate of 10°C/min under N_2 atmosphere. The value of X_C was calculated as

the ratio between the measured enthalpy value (ΔH_m), normalized with respect to the actual content of PVDF in the composite films, and enthalpy of fusion of a perfect PVDF crystal (ΔH_0 = 104.6 J/g). [36]

The density of composites was measured by the Archimedes' method. The relative density was calculated as the ratio between the measured density and the calculated theoretical density and is expressed in percentage values. The theoretical density was calculated as in [38], using the appropriate volume fraction of filler, crystallinity degree, and relative amount of electroactive phases of PVDF and using 5.965 g/cm^3 as filler density, as measured by Micrometrics Instrument Corporation AccuPycTM 1330 helium pycnometer. Optical properties of the prepared systems were investigated in the wavelength range 200–1400 nm using Shimadzu 2600 UV-vis spectrophotometer. Flexible films were prepared for the electrical characterization by applying the silver electrodes with silver paint (PEMCO, with organic solvent, Alfa Aesar). The prepared films were afterwards characterized from dielectric, ferroelectric and anelastic point of view.

Dielectric measurements were carried out in the temperature range 100-430 K and frequency range 0.2 kHz - 1 MHz with an HP4284A meter, by using a four wire probe. Measurements were performed on samples placed in a modified Linkam HFS600E-PB4 stage during heating and cooling at 1.5-2 K/min. The anelastic measurements were performed in the temperature range 130-400 K by measuring the complex dynamic elastic modulus $M = M' + iM''$ in the kHz range with the free flexural resonance method. Strips about 30 mm long were cut from the films, suspended on two thin thermocouple wires in high vacuum or 0.1 mbar He below room temperature and electrostatically excited on their flexural modes. The strips were made conductive with Ag paint in correspondence with the electrode and for shorting the

thermocouple. At least the 1st and 3rd modes could be alternately excited during the same experiment, probing two or more frequencies in the ratio 1:5.4 and higher [43]. For ferroelectric characterization a Precision Multiferroic Test System with High Voltage Interface-Radiant Technologies, Inc. was employed up to 4000 V. The polarization curves were measured at different external electric fields.

2.3. Poling, film assembly and testing

Electrical poling of the samples was performed in a silicon bath at 135 ^{o}C for 40 min and cooled down to 50 ^{o}C under the electrical field of 50 kV/cm in the parallel plate configuration. Poled flexible films with 1.5 cm^2 area, were wired and integrated in the Kapton tape (polyimide film) flexible cover as an insulation and protection layer. Since it remains stable under the wide range of temperatures -269 - +400 ^{o}C and has a high isolation ability, Kapton is usually used in the flexible electronic industry, for aircrafts, spacecrafts etc. Testing on force impact was carried out using Quartz Impulse hammer with IEPE output modal, KISTLER, Italy.

3. Results and discussion

3.1. Characterization of active phase powders

The formation of the pure perovskite structure of NBT-BT solid solution has been assessed by the X-ray diffraction (XRD). Fig. 1a shows the XRD pattern of the as-calcined NBT-BT (with 6% BT) powders confirming the formation of the desired perovskite structure at morphotropic phase boundary. The particles of NBT-BT powders used for the preparation of composite flexible films were morphologically characterized by scanning electron microscopy

(SEM). The inset of Fig. 1a displays SEM image of NBT-BT particles, where aggregates of particles of nanometer size ~ 100 nm can be observed.

3.2. Characterization of composite NBT-BT-PVDF flexible films

One of the prepared NBT-BT-PVDF films is presented in the photograph of Fig. 1c. All the flexible films were in the shape of disks with diameter around 3-4 cm and showed good flexibility. As the amount of inorganic active phase in the polymer matrix increases the film becomes less flexible, as expected.

Morphological SEM analysis of the NBT-BT-PVDF flexible films was carried out. SEM micrographs of the external surface and transversal internal surface of the sample NBT-BT-PVDF35 are reported in Fig. 1b. The following trend was observed, the lower the NBT-BT content, the more uniform the distribution of the filler is. In each film, small areas with predominantly PVDF polymer phase were noticed. The thickness of the films can be also determined from the micrographs and ranges from 110, 150 and 200 μm respectively with the increase of active component concentration in the film.

In order to investigate the influence of the hot pressing method on phase composition in PVDF, for comparison, neat PVDF film was also prepared by this method. XRD results of neat PVDF film were compared with the results of commercial PVDF powder, used for the preparation of flexible films (Fig. 2a). The PVDF powder is mainly composed of α-phase, as evidenced by two intense diffraction peaks at 18.4 and 20.0 and weaker one at 26.6, corresponding to (020), (110) and (021) reflections of the monoclinic α-phase crystal, respectively. On the other hand, XRD of the neat PVDF flexible film, besides these three peaks, possesses a peak at 20.6 corresponding to 110/200 reflection of the orthorhombic β-phase,

proving that the appearance of the β-phase was induced by the hot pressing procedure. This was an indication that electroactive polymeric phases could be present in the composite films and therefore investigation on the relative amount of PVDF polymorphs was conducted for all flexible composite films [44].

Allowing the individuation and quantification of the most important crystalline phases, infrared spectroscopy was found to be a very useful and precise technique to study the polymorphism of the PVDF matrix [36]. The ATR-FTIR analysis (Fig. 2b) confirms and complements the XRD results. The PVDF powders are indeed characterized by a neat predominance of the α phase, where the principal peaks characteristic of this non-polar polymorph at 1423, 1383, 1209, 1149, 975, 854, 795, 763, 614, 532, 489, and 410 cm^{-1} are clearly visible. The processing of the polymer induces the formation of electroactive phases, indicated by the peaks around 840 cm^{-1} in the spectrum of the PVDF hot pressed film; the co-presence of the bands at 811 and 1234 cm^{-1}, ascribed to the γ-phase, and those at 443 and 1275 cm^{-1}, exclusive of the β-phase suggests that both the polar polymorphs are simultaneously present.

Also, all the flexible NBT-BT-PVDF composites were subjected to spectroscopic characterization. The broad band around 525 cm^{-1}, whose intensity increases by increasing the filler amount, is due to the NBT-BT, and, in particular, to the metal-oxygen (M-O) stretching vibrations. In all the composites the peaks characteristic of the two electroactive phases (*i.e.*, β and γ) are identifiable but with a different intensity depending on the film composition. Regarding to that, Equation 1 was used to derive the amount of α (F_α), and electroactive phases, β (F_β) and γ phases (F_γ) which are reported in Table 1. It seems that the highest amount of

electroactive phases is found in the NBT-BT-PVDF30 sample 65%, of which 45% of the most desirable ferroelectric β-phase [34, 42, 45-47].

The ATR-FTIR results are in accordance with the calorimetric analysis. The DSC thermograms are reported in Fig. S2. Despite the melting behavior of PVDF depends not only on the polymorphism but also on other characteristics such as crystalline size and defects, a range of melting temperatures for the different crystalline phases is reported in the literature [32]; in particular, the β-crystallites show a melting temperature similar to that of α-form while, when the γ phase is obtained crystallization from the melt as in the present case, its melting peaks is about 8°C higher than that of the other two polymorphs.

The DSC thermograms, reported in Fig. S2, show that in the case of the hot-pressed PVDF and its composite containing 40Vol% of BNBT, which both are characterized by a larger amount γ phase, the polymer melting curve exhibits beside the main peak centered at about 160°C a clearly visible shoulder at higher temperatures (about 170°C).

Since Equation 1 allows calculating the relative amount of the crystalline phases without taking into account the overall quantity of PVDF crystalline phase with respect to the amorphous counterpart, the crystallinity degrees of the samples were calculated as well. As visible from Table 1, the presence of the particles reduces the overall crystallinity degree of PVDF, but, being the X_c values comparable for all the composites, the trends observed for the different polymorphs remain valid.

Mohanty et al. [47] have shown that the negative electrostatic charge of nanoparticles of the filler is used to potentiate the nucleation of β-phase in PVDF. These authors worked on the NBT-BT-PVDF films obtained by the solution casting method and pointed out that the negatively charged surface of the NBT-BT, confirmed by the zeta potential measurement,

enabled mostly the formation of β-phase. Actually, the CH_2 bonds of the PVDF and the negatively charged surface of NBT-BT particles have a strong interaction, which induced extended TTTT conformation aligned on the surface of nanoparticles and resulted in the formation of the β-phase [31, 34, 47]. It was also demonstrated that there is possibly a critical limit of filler amount that leads to the restricted formation of β-phase. After a certain concentration of filler, particles begin to be prone to agglomeration and thus the ionic dipole interactions are getting weaker and the number of centers for the nucleation of β-phase decrease. The results obtained in the investigated case are partially in agreement with the data obtained from Mohanty *et al*. Here, the presence of NBT-BT filler in the polymer matrix indeed potentiates the formation of β-phase in the films; however, the amount of β-phase decreases with filler amount probably due to differences in the methods used for the preparation of the films in compared studies [47]. Notwithstanding this, the existence of electroactive β-phase in the film will surely improve its electrical properties and broaden its possible applications.

The UV-VIS optical absorption was measured for the starting NBT-BT and PVDF powders as well. It can be suggested that there is a strong electrostatic interaction between the filler and PVDF matrix, which affects the electronic transition between the valence band and conduction band of NBT-BT filler, influencing the electronic properties of the composite films. Detailed explanations are given in the supplementary material [47-52] and Fig. S1.

Since NBT-BT ceramic filler and PVDF polymer are materials with significantly different properties, the electrical properties of their composites are influenced not only by the relative permittivity of the polymer and the filler, but also by other factors such as the morphology of the filler, its dispersion, volume fraction of the filler, structural defects and pores, the existence of different molecular conformations of PVDF and interactions between the

obtained phases [2, 47, 53, 54]. It is also important to note that in flexible films consisting of functional material embedded in a polymer matrix, the effective distance between the electrodes and effective electrode area can vary (due to small variations of the film thickness) and can complicate the interpretation of the electric and ferroelectric experimental data.

The temperature dependence of the dielectric permittivity, ε` and loss tangent, tan δ at different frequencies of the flexible composites and neat PVDF are presented in Fig. 3a-d. The dielectric permittivity value of each composite is lower in comparison with NBT-BT (6% BT) dielectric permittivity value, which is about 2000 [25-26] but higher than dielectric permittivity of neat PVDF film ~ 10 [7, 36].

There is an effect of the increase of the active phase concentration in the film: the dielectric permittivity for 40 vol% is nearly two times higher than for 30 vol% and eight times higher than for neat PVDF, while the losses at room temperature (measured at the standard frequency of 1 kHz) remain below 3 % (Fig. 4a-b). Although the dielectric permittivity around ~ 80 obtained for these samples is much smaller than that of NBT-BT, it is however a much higher value in comparison with similar composites reported in other works [47, 55-59].

This is illustrated in the Table 2, where a comparison of dielectric permittivity and loss (at RT and frequency 1 kHz) from various lead-free ferroelectric ceramics/PVDF compositions is given. Results reported in the literature have been selected for those compositions with relatively low dielectric loss tangent. Higher amount of NBT-BT filler results into poorer dispersion in the polymer which is followed by the formation of more structural defects and pores in the composite. The existing literature data suggested rather different concepts regarding dielectric properties of different PVDF polymorphs in neat films. The main issue is that different processing methods can tune the polymorphism of PVDF films and change the characteristics of

the polymer such as: the degree of crystallinity, the polymer chains orientation, the size of the crystals etc. In this regard, besides the effect of the amount of NBT-BT filler on dielectric properties, the type of PVDF polymorphism formed in the flexible film was also considered as important factor (see FT-IR results). W. Xia *et al.* who presented the study about PVDF polymers and its properties prepared by casting and further quenching, suggested that non polar α- phase possesses higher dielectric permittivity than β-and γ-PVDF phases [34]. Similarly, S. Muduli *et al.* have shown in their work, in which neat PVDF films were prepared by solvent casting and later hot pressing, that an increase of β-phase fraction reduces the dielectric constant [44]. On the contrary, R. Gregorio *et al.* prepared melting solution casted PVDF films and noticed that in the samples with predominantly β-phase the dielectric permittivity was higher [60]. Yang *et al.* solvent casted PVDF films and passed them through the roller machine in order to increase their β-phase content, pointing that films with higher amount of β-phase possessed enhanced dielectric properties [41].

In our case, sample NBT-BT-PVDF 30 has the lowest value of ε`, having the lowest amount of filler but also the highest concentration of β-phase among all composites. Even though the specimen NBT-BT-PVDF 40 possesses the lowest amount of β-phase, its dielectric permittivity value is the highest. The results show that there is an increasing trend in dielectric permittivity with β-phase fraction decrease. However, it seems that the dielectric permittivity value of all obtained composites is mostly affected by the filler amount rather than the crystalline phases formed in the films [34, 54]. The dielectric permittivity values for all samples are almost frequency independent in the low temperature region (up to 200 K), but above this temperature, a region of dispersion emerges. The most prominent dielectric dispersion can be seen for temperatures between 200 and 350 K. The main feature is the shift of the maximum of dielectric

loss toward higher temperatures with the increase of the measurement frequency, which should be due to the effect of freezing of dipolar motion in the amorphous PVDF matrix. This can be noticed for the neat PVDF and all composite films as well [7]. The dielectric response of the composites in this region is mainly determined by the response of the PVDF polymer and its glass transition [7, 61].

By a closer look, one can also register a very useful zone around room temperature as a plateau with relatively constant dielectric permittivity and losses. The broad relaxor peak characteristic for the NBT-BT (6% BT) ceramics expected in the region between 400-550 K is missing from the dielectric spectrum since it is out of the measurement range [25-26, 62]. Despite that, the tangent losses of all composites start curving down above 400 K which may be correlated with the dielectric relaxation caused by the NBT-BT filler. Some authors suggested that this relaxation can be attributed also to the wide oscillation angle of polymer polar groups followed by their rotation with main chain co-operation [2, 7].

Fig. 4a-b shows the results obtained from dielectric spectroscopy measurements for these systems at ambient temperature. The frequency variation of the dielectric permittivity and dielectric loss tangent in the frequency range 20 Hz-1 MHz are displayed for the neat PVDF and composite flexible films. It can be observed that the dielectric permittivity for neat PVDF and film with the lowest amount of the filler is almost constant in the whole frequency region. On the other hand, the dielectric permittivity for NBT-BT-PVDF35 and NBT-BT-PVDF40 shows rapid increase with lowering frequency (starting from around 10 kHz), probably due to increased conductivity in the material. The dielectric loss tangent preserves a low value (a few percent) and it is nearly constant in the whole frequency range for pure PVDF and NBT-BT-PVDF 35 and 40

samples. The NBT-BT-PVDF30 films have shown unexpected behavior, with quick increase also below 10 kHz.

For anelastic measurements three strips were cut from circular films of NBT-BT-PVDF30, 35 and 40 and excited on their flexural modes. The fundamental resonance frequency is:

$$f_1 = 1.028(t/l^2)(E/\rho)^{1/2}, \qquad (2)$$

where t, l, E and ρ are the sample thickness, length, Young's modulus and density. The Young's modulus was evaluated from this formula with an error of up to 20% due to the non-uniform thickness, especially for the 35% sample. The elastic energy loss, or reciprocal of the mechanical quality factor, $Q^{-1} = E''/E'$, was evaluated from the width of the resonance curves. Higher frequencies were probed by exciting during the same temperature run the 3rd flexural mode, with $f_3 \cong 5.4 f_1$ and higher modes when possible (Fig. 4c). Fig. 4d presents the temperature dependence of the Young's modulus and elastic energy loss of NBT-BT-PVDF40 measured on three flexural modes during heating. The curves are relatively stable, and the gray line had been obtained three days before on cooling. The temperature dependence of the Young's modulus and the losses are dominated by those of the polymer, but the magnitude of the modulus is larger of a factor ~3 with respect to PVDF due to the rigid ceramic fraction, similarly to the dielectric permittivity [7].

All the three major Q^{-1} peaks and the corresponding steps in the modulus shift to higher temperature with increasing frequency and certainly correspond to those in the dielectric permittivity (the permittivity, ε should be compared with $1/E$). Table 2 summarizes the density, measured with Archimedes method, the fundamental resonance frequency at room temperature and the corresponding Young's modulus of the three compositions. Notice that the resonance frequency depends considerably on T, for example from 212 Hz to 650 Hz with cooling for the

40% sample. As expected, there is stiffening with increase of the ceramic fraction. The local minimum of *E* at 35% is within the experimental error due to the non-homogeneous thickness, but also reflects a minimum in density.

P-E hysteresis loops of pure PVDF and its composites measured at room temperature, at 170 kV/cm and frequency of 100 Hz are presented in Fig. 5a. The hysteresis loops are well defined but not saturated and therefore the remnant polarization values of the films cannot be compared with high accuracy. The saturation was not reached possibly due to the limitation of the voltage source (4000 V). This can be seen in the literature quite often for the composite films made of PVDF with other different fillers, such as, PZT, PLZT, BT, NBT etc. [2, 22, 54, 63, 64]. Fig. 5b presents the polarization vs. electrical field at the highest reached field for each sample (limitation of the equipment). The values of the maximum reached field decrease with the increasing concentration of active phase, due to the fact that the films with higher concentration of the filler were thicker, resulting in a lower field under the same voltage. Many parameters can influence the ferroelectric properties such as interface areas, agglomerations, voids in the composites, inhomogeneous distribution of filler in the polymer matrix etc. [2, 63, 64]. However, as mentioned previously, there are a couple of more important effects that can influence the ferroelectric properties of these composite materials and have to be considered. The sintered NBT-BT ceramics possesses good ferroelectric properties with nicely saturated square shaped hysteresis loop measured at 50 kV/cm with $P_r = 38\ \mu C/cm^2$ and $E_c = 30$ kV/cm (inset of Fig. 5a), which is in agreement with the data available from the literature [65-66].

Likewise, the literature about ferroelectric properties of pure α, β and γ PVDF films points to the possibility of a profound effect of PVDF phases on the ferroelectric properties of the composites [33-34, 46-47, 54, 67]. Neat β- phase PVDF shows typical characteristic of

normal ferroelectric in the squared shaped loops for its all-trans conformations. α- and γ- PVDF phases have smaller remnant polarization under the same conditions, and P_r of γ-PVDF is slightly higher than that of α-PVDF which can be attributed to the T3G conformation which is more polar than TGTG` of α-PVDF [33-34].

Thus, as it can be noticed from Fig. 5a-b, in our case there is a combined effect of both, influence of the filler amount and effect of PVDF crystal phases present in each film. The NBT-BT-PVDF30 has the lowest amount of the filler but also the highest concentration of the ferroelectric β- phase, 45% and it shows a bit lower P_r and E_c values in comparison with the NBT-BT-PVDF35 sample that has 32 % of β- phase but a higher concentration of the filler.

The largest loop area which is connected with high losses can be seen for the NBT-BT-PVDF40 sample that possesses the highest amount of filler but the lowest concentration of the ferroelectric β- phase ~7%.

3.3. Application point of view: Energy storage and Energy harvesting

Energy storage

During the recent years researchers have been studying PVDF based composites reinforced with various fillers, e.g., PZT, BT, BST, TiO_2 etc. for developing energy storage materials [42, 54, 64, 68, 69]. As demonstrated here and in the literature [47-69], ceramic fillers and PVDF polymer have very different properties, with advantages and disadvantages. In order to develop a good material for the energy storage application with high energy density, the above mentioned excellent properties of each material, organic polymer and ceramic filler, can be combined by the preparation of polymer composites.

Here regarding the resulting dielectric and ferroeletric properties of the flexible composites, the potential of these materials for the energy storage application was investigated.

As it was presented, the NBT-BT ceramic filler exhibits much higher values of dielectric permittivity in comparison with PVDF polymer, affecting the increase of the overall dielectric permittivity of the composite material. However, introduction of the ceramic filler in the polymer matrix also causes formation of different defects and pores in the structure and lowers the flexibility and the electric breakdown strength of the composite [47,53,54]. It can be noticed that the electric breakdown strength is affected by the amount of the ceramic filler in the composite. As the amount of the filler increases, more inhomogeneous distribution of the filler in the polymer occurs; more voids and defects are formed, causing the local electric field concentration increase and contemporary reduction of the breakdown strength of the composite materials in comparison with neat PVDF [70]. Due to the limits of the used instrumentation, the electric breakdown strengths values for each composite was not reached, but from the E_{max} presented in the Table 3 it can be concluded that the amount of filler surely affects the properties necessary for the energy storage application.

In the general terms, the energy storage density of a dielectric material can be described by the equation:

$$J=\int_{Dr}^{Dmax} E\, dD\ , \qquad (3)$$

where D_{max} and D_r are the maximum of the electric displacement and remnant electric displacement and E is the electric field [42, 71]. The energy storage density represents the electrical energy stored in a unit volume of the dielectric material [42, 54]. The electric displacement D is a very important factor in achieving high values of energy density. It has to be high enough, but along with low remnant polarization value [42]. Typical electric displacement-electric field loops at 170 kV/cm for all investigated films, are presented in the Fig. 5c. It can be noticed that as the amount of filler increased, the electric displacement notably increased and

reached the highest value of 2.30 μC/cm^2 for the NBT-BT-PVDF40 sample. According to the formula D= $\varepsilon_0\varepsilon`$E, where $\varepsilon_0$ is the dielectric permittivity of the vacuum, $\varepsilon`$ is the relative dielectric permittivity and E is the electric field, the rise of dielectric permittivity of the composite can be related to the electric displacement increase. Derived values for energy density (from the surface above the D-E curve) presented in the Table 3 at the field of 170 kV/cm show that the energy density became higher with the amount of NBT-BT filler in the polymer matrix. The energy density is getting higher with the increase of electric field as well, and for the same sample NBT-BT-PVDF35 changes from 0.108 J/cm^3 at 170 kV/cm to 0.172 J/cm^3 at 210 kV/cm. In ferroelectrics, due to the presence of electric hysteresis and remnant polarization, the electrical energy stored in the material is not completely released and due to the energy losses (the closed part of the loop) the energy density is low [54]. Therefore, besides high energy density, for the practical application in the energy storage devices, it is important that the material possesses high efficiency. The energy efficiency $\eta=J/(J+J_{loss})$, where J and J_{loss} are energy density and energy loss, can be obtained from the D-E loops. Energy density efficiencies obtained for investigated materials are presented in the Table 3, showing a decreasing trend with increasing amount of NBT-BT. However the values of 66-74 % that were obtained for all investigated composites, according to other authors, are enough for the practical application of these materials [42, 47, 54]. Low leakage current density is also an important parameter for the application of the material for energy storage. Leakage current density (*j*) was measured as a function of static electric-field (*E*) in order to study the conductivity in the material and it is presented in Fig. 5d. Keeping in mind that the leakage current is related to the electric conductivity, the obtained results imply the highest electrical conductivity of the NBT-BT-PVDF40 which is followed by slight decrease for the samples NBT-BT-PVDF30 and NBT-BT-PVDF35, respectively.

Significantly lower leakage current density was measured for neat PVDF flexible film. Since both component phases, PVDF and NBT-BT, show low conductivity, it means that the conductive channels are created in the composite phase. Indeed, as it was suggested earlier, the amount of ceramic filler can cause the formation of more defects, pores and space charge in the composite, and worsen the mechanical properties and flexibility, provoking the increase of the leakage current density [2, 23, 67, 70].

Energy harvesting

Different types of mechanical energy can be harvested from the surrounding environment such as bending, pushing, acoustic waves, mechanical vibrations, wind and human activities. The trend today is to use surfaces of buildings, roads, soccer fields, train stations, school corridors as green areas, for energy production or for some other useful purpose [9, 34, 53].

Piezoelectric materials are the group of materials that can generate charge when mechanical stress is applied. According to their structure they can be divided into four different categories: ceramics, single crystals, polymers and composites [72].

During the years, numerous studies on all types of piezoelectric materials were carried out in order to develop energy harvesting elements. A family of lead based materials, PZT and its various modifications, are the materials that have shown excellent piezoelectric performance, and are the most frequently used materials for this application [1-11]. Due to necessity for the removal of lead from all consumer items, a pursuit for lead-free substitutes that can compete with lead-containing materials has begun. Polymer piezoelectric materials, such as PVDF and its copolymers, have been very often used as energy harvester elements for wearable items, in fluids and air, as a result of their flexibility and bendability. However, piezoelectric polymers typically

provide lower power output in the micro Watt range, smaller in comparison with the piezo-ceramic energy harvester based on PZT [72].

In order to combine good piezoelectric properties of the ceramics and flexibility of the polymers, composites consisting of ceramic filler incorporated in the polymer matrix are being developed extensively during the last decade. However, piezoelectric properties of the used filler, usually PZT based, are getting diluted as the polymer matrix represents the majority of the material. It is very important that films possess maximum amount of the piezoelectric filler while retaining its flexibility, that enables that these composite films can respond much faster than ceramics ones [4,27,72,73].

In this study, poled lead-free flexible films were electroded with silver and wired with Cu wires in order to enable the connection with external circuit. The energy harvester unit was encapsulated in the two layers of thin Kapton tape which is a protective layer and gives dimensional stability to the device (see Fig. 6b).

In order to achieve uniform distribution of mechanical stress on the sample, the sample was placed in the holder between sandwich like metal plates with two springs at the ends of the bottom plate. Thus, after each mechanical impact of impulse hammer, springs were able to return the upper metal plate into the original position. The scheme of the testing set-up with all used mechanical and measuring equipment was presented in Fig. 6a. Voltage generation of polymer/ceramic composites NBT-BT-PVDF30/35/40 while applying the impact force of 250 N are presented in Fig. 6c. The highest value of the output voltage was 8-9 V for NBT-BT-PVDF30, 4-5 V for NBT-BT-PVDF35 and around 1.5 V for NBT-BT-PVDF40. The highest values of output current ~ 8-9 μA and maximum of generated power up to 81 μW were obtained

for the NBT-BT-PVDF30. Accordingly, lower values were achieved for other two samples and the lowest voltage output was found in the neat PVDF flexible films ~ 1 V.

The explanations for the voltage output decrease with filler amount increase can be the agglomeration of filler particles and non-completely homogeneous distribution of the filler in the polymer matrix, supported by the literature data [22, 47,70,72] and proven by measured density values of the composites. On the other hand, another possible explanation could be found in PVDF polymorphism. According to the literature data, with the poling method used in this study, in which PVDF films were under the influence of high field and high temperature for almost 1.5 h, polymorphic changes of PVDF are expected [32, 34, 42, 47]. The FT-IR analysis (performed before and after poling) indicates a lowering of the sum of electroactive β- and γ- PVDF phases after poling (Fig. S3). This counterintuitive result was noticed in all films, including those with good voltage output, and may be explained by an effective contribution of the γ- phase, whose fraction increases after poling. Although, the electroactive β-phase is proven to show the best piezoelectric response among the other phases, this investigation may shed light also on the importance of the electroactive γ- phase in the films. These enhanced properties in the NBT-BT-PVDF30 can be attributed to a higher amount of electroactive phases and better distribution of the filler in this flexible composite. Additionally, the piezoelectric charge constants, d_{33}, were determined using the equation: d_{33}= -C*V/F, where C is the capacitance of the film (pF), V is the output voltage (V) and F is the applied force (N) [74-75]. The values obtained were 16; 7 and 2 pC/N for NBT-BT-PVDF30/35/40 samples, respectively and 2 pC/N for neat PVDF film. The results are in accordance with the measured output voltage values.

However, the issue of polymorphism changes could be probably solved by the corona poling method, in which PVDF samples are exposed to extreme poling conditions for a short period of time, which is not enough for significant changes in the polymer structure [75-76].

Future work will be focused on the resolving the problems induced by the poling conditions and its effect on the energy harvesting performance of the NBT-BT-PVDF30 composite films.

Conclusion

Flexible polymer/ceramics composite films were successfully prepared by the adding lead-free piezoelectric material sodium bismuth titanate-barium titanate (NBT-BT) in the polymer polyvinylidene fluoride (PVDF) matrix by hot pressing. Flexible films with different filler amount were prepared and investigated. Detailed structural analysis of films leads to the conclusions that the hot pressing method partially induced the formation of electroactive β-phase of PVDF polymer, influencing in that way the electrical properties of the material. Even NBT-BT as filler with negatively charged surface can favor a predominant formation of desirable piezoelectric PVDF phase. The dielectric permittivity of the films obtained in this study was much higher in comparison with the one obtained from other authors. NBT-BT-PVDF 40 had nearly two times higher values of dielectric permittivity than NBT-BT-PVDF 30 and eight times higher than neat PVDF, while the losses at room temperature (measured at the standard frequency 1 kHz) remained below 3 %. A very useful zone around room temperature as a plateau with relatively constant dielectric permittivity and losses was noticed in the dielectric spectra of each film. Anelastic measurements showed a complete agreement with dielectric properties in which the temperature dependence of the Young's modulus and the losses are dominated by

those of the polymer, but the magnitude of the modulus is larger of a factor ~3 with respect to PVDF due to the rigid ceramic fraction. Non-saturated hysteresis loops pointed out the combined effect of two factors, that is influence of the filler amount and effect of PVDF crystal phases present in each film. Calculations of energy storage density and energy density efficiencies obtained for the investigated materials revealed a decreasing trend with increasing amount of NBT-BT. The values of η= 66-74 % that were obtained for all the composites, were determined as high enough for the practical application of these materials.

Assembled energy harvesting units were made by proper wiring and covering the flexible film with a Kapton protection layer. Charge generation of polymer/ceramics composites while applying the impact force was investigated. The highest value of the output voltage was 9 V and it was obtained for NBT-BT-PVDF30 (4.5 V for NBT-BT-PVDF35 and 1.5 V for NBT-BT-PVDF40). The highest values of output current was ~ 9 μA and maximum of generated power was up to 81 μW.

The main conclusion derived from this study is that flexible composite films made of lead-free NBT-BT filler and PVDF matrix, especially NBT-BT-PVDF 30, have high potential to be used for efficient environmentally safe low-energy storage and harvesting devices.

Acknowledgement

The authors gratefully acknowledge the Ministry of Education, Science and Technological development Republic of Serbia to financial support given through national programs (project code 451-03-68/2020-14/200053) and bilateral project (project code in SR 451-03-03064/2018-09/1) “Lead-free piezoelectric and multiferroic flexible films for nanoelectronics and energy harvesting” with Italy and Ministry of Foreign Affairs and International Cooperation of Italy (project code: RS19MO01). Claudio Capiani from CNR-

ISTEC for the preparation of the NBT-BT powders and dr Maria Teresa Buscaglia from CNR-ICMATE for SEM analysis of NBT-BT powder are gratefully acknowledged.

Reference

1. Y. Lua, J. Chena, Z. Chenga, S. Zhanga, The PZT/Ni unimorph magnetoelectric energy harvester for wireless sensing applications, Energ. Convers. Manage. 2019; 200: 112084
2. J. D. Bobic, G. Ferreira Teixeira, R. Grigalaitis, S. Gyergyek, M. M. Vijatović Petrovic, M. Ap. Zaghete, B. D. Stojanovic, PZT–NZF/CF ferrite flexible thick films: Structural, dielectric, ferroelectric, and magnetic characterization. J. Adv. Ceram. 2019; 8(4): 545–554
3. A.K. Sharma, J.K. Swamy, A. Jain, Dielectric properties of PVDF-PZT composite films and their thermal dependence. Advanced Materials Proceedings 2016; 1(2): 185-190
4. S.H. Wankhade, S. Tiwari, A. Gaur, P. Maiti, PVDF–PZT nanohybrid based nanogenerator for energy harvesting applications. Energy Rep. 2020; 6: 358–364
5. S.K. Sharma, H. Gaur, M. Kulkarni, G. Patil, B. Bhattacharya, A. Sharma, PZT–PDMS composite for active damping of vibrations, Compos. Sci. Technol. 2013; 77: 42–51
6. D.P. Anh, D.V. On, D.A. Quang, N. Van Thinh, N. T. Anh Tuyet, V. Thanh Tung, T.Van Chuong, Dielectric and Piezoelectric Properties of PZT/PVDF Composites Prepared by Hot Press Method, Inter. J. Engin. Res. Technol. 2020; 9(4): 898-902
7. B. Hilczer, J. Kułek, E. Markiewicz, M. Kosec, B. Malic, Dielectric relaxation in ferroelectric PZT–PVDF nanocomposites, J Non-Cryst. Solids 2002; 305: 167–173
8. B. Li, Q. Liu, X. Tang, T. Zhang, Y. Jiang, W. Li, J. Luo, High Energy Storage Density and Impedance Response of PLZT2/95/5 Antiferroelectric Ceramics, Materials 2017; 10: 143

9. A. Jain, K.J. Prashanth, A. Kr. Sharma, A. Jain, P.N. Rashmi, Dielectric and Piezoelectric Properties of PVDF/PZT Composites: A Review, Polym. Eng. Sci. 2015; 55(7): 1589-1616
10. N. Cai, J. Zhai, C.-W. Nan, Y. Lin, Z. Shi, Dielectric, ferroelectric, magnetic, and magnetoelectric properties of multiferroic laminated composites, Phys. Rev. B 2003; 68: 224103
11. T. Siponkoski, M. Nelo, J. Palosaari, J. Perantie, M. Sobocinski, J. Juuti, H. Jantunen, Electromechanical properties of PZT/P(VDF-TrFE) composite ink printed on a flexible organic substrate, Compos. Part B 2015; 80: 217-222
12. J. Rödel, K.G. Webber, R. Dittmer, W. Job, M. Kimurac, D. Damjanovic, Transferring lead-free piezoelectric ceramics into application, J. Eur. Ceram. Soc. 2015; 35: 1659–1681,
13. H. Zhang, W. Ma, B. Xie, L. Zhang, S. Dong, P. Fan, K. Wang, J. Koruza, J. Rodel, $(Na_{1/2}Bi_{1/2})TiO_3$-based lead-free co-fired multilayer actuators with large strain and high fatigue resistance, J. Am. Ceram. Soc. 2019; 102: 6147–6155.
14. M. I. Bichurin, D. A. Filippov, V. M. Petrov, V. M. Laletsin, N. Paddubnaya, G. Srinivasan, Resonance magnetoelectric effects in layered magnetostrictive-piezoelectric composites, Phys. Rev. B 2003; 68: 132408
15. J. I. Roscow, Y. Zhang, M.J. Kraśny, R.W.C. Lewis, J. Taylor, C.R. Bowen, Freeze cast porous barium titanate for enhanced piezoelectric energy harvesting, J. Phys. D: Appl. Phys. 2018; 51: 225301
16. L.-Feng Zhu,B.-Ping Zhang, L. Zhaoa, J.-Feng Lib, High piezoelectricity of $BaTiO_3$–$CaTiO_3$–$BaSnO_3$ lead-free ceramics, J. Mater. Chem. C, 2014; 2: 4764
17. M. Cernea, L. Trupina, B.S. Vasile, R. Trusca, C. Chirila, Nanotubes of piezoelectric BNT–BT0.08 obtained from sol–gel precursor, J. Nanopart. Res. 2013; 15: 1787

18. S.-Tao Zhang, A. Brice Kounga, E. Aulbach, T. Granzow, W. Jo, H.-Joachim Kleebe, J. Rödel, Lead-free piezoceramics with giant strain in the system $Bi_{0.5}Na_{0.5}TiO_3 – BaTiO_3– K_{0.5}Na_{0.5}NbO_3$ I. Structure and room temperature properties, J. Appl. Phys. 2008; 103: 034107

19. W. Liu, X. Ren, Large Piezoelectric Effect in Pb-Free Ceramics, Phys. Rev. Lett. 2009; 103: 257602

20. Y. Liu, Y. Chang, F. Li, B. Yang, Y. Sun, J. Wu, S. Zhang, R. Wang, W. Cao, Exceptionally High Piezoelectric Coefficient and Low Strain Hysteresis in Grain-Oriented (Ba,Ca)(Ti,Zr)O_3 through Integrating Crystallographic Texture and Domain Engineering, ACS Appl. Mater. Inter., 2017; DOI: 10.1021/acsami.7b08160

21. Z. Wang, J. Wang, X. Chao, L. Wei, B. Yang, D. Wang, Z. Yang, Synthesis, structure, dielectric, piezoelectric, and energy storage performance of $(Ba_{0.85}Ca_{0.15})(Ti_{0.9}Zr_{0.1})O_3$ ceramics prepared by different methods, J. Mater. Sci.: Mater. Electron. 2016; 27: 5047-5058

22. S. Moharana, S. Sai, R. Naresh Mahaling, Enhanced dielectric and ferroelectric properties of surface hydroxylated $Na_{0.5}Bi_{0.5}TiO_3$ (NBT)-poly(vinylidene fluoride) (PVDF) composites. J. Adv. Diel. 2018; 8 (3): 1850017

23. D. Mauryaa, M. Peddigarid, M.-Gyu Kang, L.D. Geng, N. Sharpes, V. Annapureddy, H. Palneedi, R. Sriramdas, Y. Yan, H.-Cheol Song, Y.U. Wang, J. Ryub, S. Priyac, Lead-free piezoelectric materials and composites for high power density energy harvesting, J. Mat. Res. 2018; 33(16): 2235-2263

24. V. Dorcet, G. Troillard, P. Boullay, Reinvestigation of Phase Transitions in $Na_{0.5}Bi_{0.5}TiO_3$ by TEM. Part I: First Order Rhombohedral to Orthorhombic Phase Transition, Chem. Mater. 2008; 20: 5061

25. F. Cordero, F. Craciun, F. Trequattrini, E. Mercadelli, C. Galassi, Phase transitions and phase diagram of the ferroelectric perovskite $(Na_{0.5}Bi_{0.5})_{1-x}Ba_xTiO_3$ by anelastic and dielectric measurements Phys. Rev. B 2010; 81: 144124
26. F. Craciun, C. Galassi, R. Birjega, Electric-field-induced and spontaneous relaxor-ferroelectric phase transitions in $(Na_{1/2}Bi_{1/2})_{1-x}Ba_xTiO_3$, J. Appl. Phys. 2012; 112: 124106
27. F. Ru Fan, W. Tang, Z. Lin Wang, Flexible Nanogenerators for Energy Harvesting and Self-Powered Electronics, Adv. Mater. 2016; 28: 4283–4305
28. B.D. Stojanovic, A.S. Dzunuzovic, N.I. Ilic, M.M. Vijatovic Petrovic, Complex composites: Polymer matrix-ferroics or multiferroics. In B.D. Stojanovic and G. Korotcenkov, editor. Magnetic, Ferroelectric, and Multiferroic Metal Oxides. Amsterdam: Elsevier, 2018, p. 559-569.
29. L. Mateu, T. Dra¨ger, I. Mayordomo, M. Pollak, Energy Harvesting at the Human Body. In Sazonov E, editor. Wearable Sensors. Amsterdam: Elsevier, 2014, p.
30. D. Lolla, M. Lolla, A. Abutaleb, H.U. Shin, D. H. Reneker, G.G. Chase, Fabrication, Polarization of Electrospun Polyvinylidene Fluoride Electret Fibers and Effect on Capturing Nanoscale Solid Aerosols, Materials 2016; 9: 671
31. L.Ruan, X.Yao, Y. Chang, L. Zhou, G. Qin, X. Zhang, Properties and Applications of the Phase Poly(vinylidene fluoride), Polymers 2018; 10: 228
32. P. Martins, A.C. Lopes, S. Lanceros-Mendez, Electroactive phases of poly(vinylidene fluoride): Determination, processing and applications, Prog. Polym. Sci. 2014; 39: 683–706
33. PyzoFex, PVDF and its copolymers**,** JOANNEUM RESEARCH**,** Institute for Surface Technologies and Photonics, https://www.pyzoflex.com/downloads
34. W. Xia, Z. Zhang, PVDF-based dielectric polymers and their application in electronic materials, IET Nanodielectrics Rev. 2018; 1: 17-31

35. F. Khan, T. Kowalchik, S. Roundy, R. Warren, Stretching-induced phase transitions in barium titanate-poly(vinylidene fluoride) flexible composite piezoelectric films, Scripta Mater. 2021; 193: 64–70

36. E. Brunengo, G. Luciano, G. Canu, M. Canetti, L. Conzatti, M. Castellano, P. Stagnaro, Double-step moulding: An effective method to induce the formation of β-phase in PVDF, Polymer 2020; 193: 122345.

37. E. Brunengo, M. Castellano, L. Conzatti, G. Canu, V. Buscaglia, P. Stagnaro, PVDF-based composites containing PZT particles: How processing affects the final properties, J. Appl. Polym. Sci. 2020; 137: 48871.

38. E. Brunengo, L. Conzatti, I. Schizzi, M.T. Buscaglia, G. Canu, L. Curecheriu, C. Costa, M. Castellano, L. Mitoseriu, P. Stagnaro, V. Buscaglia, Improved dielectric properties of poly(vinylidene fluoride)–$BaTiO_3$ composites by solvent-free processing, J. Appl. Polym. Sci. 2021; 138: e50049

39. B. Chu, X. Zhou, K. Ren, B. Neese, M. Lin, Q. Wang, F. Bauer, Q.M. Zhang, A dielectric polymer with high electric energy density and fast discharge speed, Science 2006; 313: 334-336

40. H.-J. Ye, L. Yang, W.-Z. Shao, S.-B. Sun, L. Zhen, Effect of electroactive phase transformation on electron structure and dielectric properties of uniaxial stretching poly(vinylidene fluoride) films, RSC Adv. 2013; 3: 23730–23736

41. L. Yang, J. Qiu, K. Zhu, H. Ji, Q. Zhao, M. Shen, S. Zeng, Effect of rolling temperature on the microstructure and electric properties of β-polyvinylidene fluoride films, J. Mater. Sci. Mater. Electron. 2018; 29: 15957–15965

42. X. Cai, T. Lei, D. Sun, L. Lin, A critical analysis of the α, β and γ phases in poly(vinylidene fluoride) using FTIR, RSC Adv. 2017; 7: 15382–15389

43. F. Cordero, L. Dalla Bella, F. Corvasce, P. M. Latino and A. Morbidini, An insert for anelastic spectroscopy measurements from 80 K to 1100 K, Meas. Sci. Technol. 2009; 20; 015702
44. S.P. Muduli, S Parida, S.K.Rout, S. Rajput, M. Kar, Effect of hot press temperature on β-phase, dielectric and ferroelectric properties of solvent casted Poly(vinyledene fluoride) films, Mater. Res. Express 2019; 6: 095306
45. M. Bohle´n, K. Bolton, Conformational studies of poly(vinylidenefluoride), poly(trifluoroethylene) and poly(vinylidene fluoride-co-trifluoroethylene) using density functional theory, Phys. Chem. Chem. Phys. 2014; 16: 12929
46. N. Meng, X. Zhu, R. Mao, M. J. Reece, E. Bilotti, Nanoscale interfacial electroactivity in PVDF/PVDF-TrFE blended films with enhanced dielectric and ferroelectric properties, J. Mater. Chem. C 2017; 5: 3296
47. H.S. Mohanty, Ravikant, A. Kumar, P.K. Kulriya, R. Thomas, D.K. Pradhan, Dielectric/ferroelectric properties of ferroelectric ceramic dispersed poly(vinylidene fluoride) with enhanced β-phase formation, Mater. Chem. Phys. 2019; 230: 221-230
48. S. El-Sayed, Optical properties and dielectric relaxation of polyvinylidene fluoride thin films doped with gadolinium chloride, Physica B 2014; 454: 197–203
49. I. Noor Bhatti, M. Banerjee, I. Noor Bhatti, Effect of Annealing and Time of Crystallization on Structural and Optical Properties of PVDF Thin Film Using Acetone as Solvent, IOSR J. Appl. Phys. (IOSR-JAP) 2013; 4: 42-47
50. L. Donga, X.-Dong Liua, Z.-Rong Xionga, D.-Kun Shenga, Y. Zhoua, Y-Ming Yang, Preparation and Characterization of UV-absorbing PVDF Membranes via Pre-irradiation Induced Graft Polymerization, Chinese J. Polym. Sci. 2019; 37: 493–499

51. J. Tauc, R. Grigorovici, A. Vancu, Optical Properties and Electronic Structure of Amorphous Germanium, Phys. Stat. Sol. 1966; 15: 627-637
52. E.A. Davis, N.F. Mott, Conduction in Non-crystalline Systems V. Conductivity, Optical Absorption and Photoconductivity in Amorphous Semiconductors, Philos. Mag. 1970; 22: 0903-0922.
53. A. Jain, K.J. Prashanth, A.K. Sharma, Dielectric and piezoelectric properties of PVDF/PZT composites: A review. Polym. Eng. Sci. 2015; 55: 1589–1616.
54. Y. Wang, M. Yao, R. Ma, Q. Yuan, D. Yang, B. Cui, C. Ma, M. Liu, D. Hu, Design strategy of barium titanate/polyvinylidene fluoride-based nanocomposite films for high energy storage, J. Mater. Chem. A 2020; 8: 884-917
55. S. Hajra, S. Sahoo, R. N. P. Choudhary, Fabrication and electrical characterization of (Bi0.49Na0.49Ba0.02) TiO3-PVDF thin film composites, Journal of Polymer Research 26 (2019), 14, 1-11.
56. J. Fu, Y. Hou, M. Zheng, Q. Wei, M. Zhu, H. Yan, Improving Dielectric Properties of PVDF Composites by Employing Surface Modified Strong Polarized BaTiO3 Particles Derived by Molten Salt Method, ACS Appl. Mater. Interfaces 7 (2015), 24480−24491.
57. Z. M. Dang, H. Y. Wang, B. Peng, C. W. Nan, Effect of BaTiO3 Size on Dielectric Property of BaTiO3/PVDF Composites. J.Electroceram. 21 (2008) 381−384.
58. P. Mishra, P. Kumar, Dielectric Properties of Φ(BZT-BCT)-(1−Φ) Epoxy Composites with 0-3 Connectivity, Advances in Condensed Matter Physics, Volume 2013 (2013), Article ID 858406, 1-9 (http://dx.doi.org/10.1155/2013/858406).
59. S. A. Riquelme, K. Ramam, Dielectric and piezoelectric properties of lead free BZT-BCT/PVDF flexible composites for electronic applications, Mater. Res. Express 6 (2019) 11633, 1-11.
60. R. Gregorio, E.M. Ueno, Effect of crystalline phase, orientation and temperature on the dielectric properties of poly(vinylidene fluoride) (PVDF), J.Mater. Sci. 1999; 34: 4489 – 4500
61. J. Banys, R. Grigalaitis, A. Mikonis, J. Macutkevic, P. Keburis, Distribution of relaxation times of relaxors: comparison with dipolar glasses, Phys. Status Solidi C 6, 2009; 12: 2725–2730

62. F. Cordero, F. Trequattrini, F. Craciun, E. Mercadelli, C. Galassi, Elastic and dielectric measurements of the structural transformations in the ferroelectric perovskite $(Na_{1/2}Bi_{1/2})_{1-x}Ba_xTiO_3$, Solid State Phenom. 2011; 172-174: 161-165

63. W. Ji, H. Deng, C. Guo, C. Sun, X. Guo, F. Chen, Q. Fu, The effect of filler morphology on the dielectric performance of polyvinylidene fluoride (PVDF) based composites, Compos. Part A-Appl. S. 2019; 118: 336–343

64. W. Nian, Z. Wang, T. Wang, Y. Xiao, H. Chen, Significantly enhanced breakdown strength and energy density in sandwich-structured NBT/PVDF composites with strong interface barrier effect, Ceram. Int. 2018; 44: S50-53

65. O. Turki, A. Slimani, , L. Seveyrat, G. Sebald, V. Perrin, Z. Sassi, H. Khemakhem, L. Lebrun, Structural, dielectric, ferroelectric, and electrocaloric properties of 2% Gd_2O_3 doping $(Na_{0.5}Bi_{0.5})_{0.94}Ba_{0.06}TiO_3$ ceramics, J. Appl. Phys. 2016; 120: 054102

66. M. Chena, Q. Xub, B. Hee Kima, B. Kuk Ahna, J. Hoon Ko, W. Jin Kang, O. Jeong Nam, Structure and electrical properties of $(Na_{0.5}Bi_{0.5})_{1-x}Ba_xTiO_3$ piezoelectric ceramics, J. Eur. Ceram. Soc. 2008; 28: 843–849

67. H. Luo, D. Zhang, C. Jiang, X. Yuan, C. Chen, K. Zhou, Improved dielectric properties and energy storage density of oily(vinylidene fluoride-co-hexafluoropropylene) nanocomposite with Hydration epoxy resin coated $BaTiO_3$, ACS Appl. Meter. Inter. 2015; 7: 8061-8069

68. J. Nunes-Pereira, V. Sencadas, V. Correia, J.G. Rocha,S. Lanceros-M´endez, Energy harvesting performance of piezoelectric electrospun polymer fibers and polymer/ceramic composites, Sensor. Actuat. A-Phys. 2013; 196: 55– 62

69. M. Ataur Rahman, B.-Chul Lee, D.-Thach Phan, G.-Sang Chung, Fabrication and characterization of highly efficient flexible energy harvesters using PVDF–graphene nanocomposites, Smart Mater. Struct. 2013; 22: 085017

70. Q. Huang, H. Luo, C. Chen, X. Zhou, K. Zhou, D. Zhang, Enhanced energy density in P(VDF-HFP) nanocomposites with gradient dielectric fillers and interfacial polarization, J. Alloy. Compd. 2017; 696: 1220-1227

71. P. Wu, M. Zhang, H. Wang, H. Tang, P. Bass, L. Zhang, Effect of coupling agents on the dielectric properties and energy storage of $Ba_{0.5}Sr_{0.5}TiO_3$/P(VDF-CTFE) nanocomposites, AIP Adv. 2017; 7: 075210

72. H. Li, C. Tian, Z. Daniel Deng, Energy harvesting from low frequency applications using piezoelectric materials, Appl. Phys. Rev. 2014; 1: 041301

73. P. Costa, J. Nunes-Pereira, N. Pereira, N. Castro, S. Gonçalves, S. Lanceros-Mendez, Recent Progress on Piezoelectric, Pyroelectric, and Magnetoelectric Polymer-Based Energy-Harvesting Devices, Energy Technol. 2019; 7: 1800852

74. Q. Guo, G.Z. Cao, I.Y. Shen, Measurements of Piezoelectric Coefficient d33 of Lead Zirconate Titanate Thin Films Using a Mini Force Hammer, Journal of Vibration and Acoustics 2013; 135: 011003-1

75. S.K. Mahadeva, J. Berring, K. Walus, B. Stoeber, Effect of poling time and grid voltage on phase transition and piezoelectricity of poly(vinyledene fluoride) thin films using corona poling, J. Phys. D: Appl. Phys. 2013; 46: 285305

76. Y. Jiang, Y. Ye, J. Yu, Z. Wu, W. Li, J. Xu, G. Xie, Study of Thermally Poled and Corona Charged Poly(vinylidene fluoride) Films, Polym. Eng Sci, 2007; 47: 1344-1350

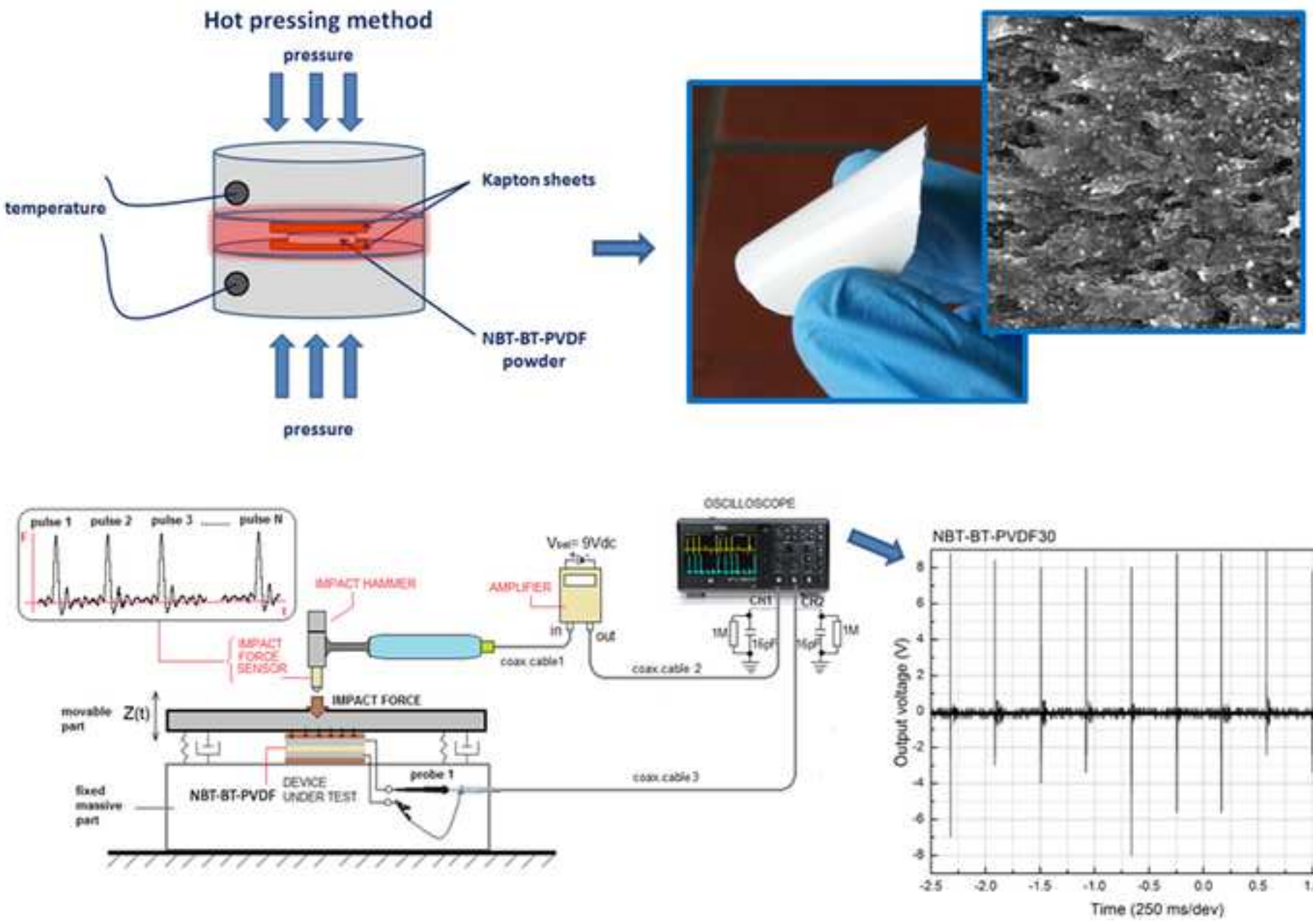

Highlights

- NBT-BT-PVDF flexible lead-free piezoelectric composite films were prepared by hot pressing.
- Hot pressing method transforms PVDF α-phase into electro-active β and γ phases.
- The dielectric permittivity increases with the active phase amount increase, up to 80.
- Notable properties both for energy storage and energy harvesting application found.
- Testing of force impact: up to 9 V and ~ 81 μW of output voltage and power obtained.

Table 1

SAMPLE	$\%F_\alpha$	$\%F_\beta$	$\%F_\gamma$	X_c
PVDF	46	4	50	50
NBT-BT-PVDF30	35	45	20	44
NBT-BT-PVDF35	50	32	18	40
NBT-BT-PVDF40	44	7	49	42

Table 2

SAMPLE	Ceramic concentr. (%)	Dielectric permittivity	Dielectric loss tan ö	Ref.
NBT-BT/PVDF	30	40	0.02	This work
NBT-BT/PVDF	35	48	0.02	This work
NBT-BT/PVDF	40	78	0.03	This work
NBT-BT/PVDF	30	11	0.05	[47]
NBT-BT/PVDF	40	10	0.03	[47]
NBT-BT/PVDF	30	18	0.03	[55]
$BaTiO_3$/PVDF	40	65	0.02	[56]
$BaTiO_3$/PVDF	40	51	0.03	[57]
BCTZ/PVDF	25	25	0.059	[58]
BCTZ/PVDF	35	22	0.025	[59]
BCTZ/PVDF	45	24.5	0.028	[59]

Table 3

x	**ρ (g/cm^3)**	**ρ (%)**	***f*$_1$ (Hz) at 295 K**	***E* (GPa) at 295 K**
30	2.96	97	230	8.2
35	3.14	97	370	7.6
40	3.21	93	420	10.5

Table 4

Sample	D ($\mu C/cm^2$)	E_{max} (kV/cm)	ε_r (at 1 kHz)	J (J/cm^3)	η (%)
PVDF	0.23	400	11	0.017	96.60
NBT-BT-PVDF30	1.06	330	40	0.0765	74.38
NBT-BT-PVDF35	1.58	260	50	0.108	68.35
NBT-BT-PVDF40	2.30	150	73	0.148	66.37

Table captions

Table 1. Amount of α (F_α), and electroactive phases, β (F_β), γ phases (F_γ) and the crystallinity degree (X_C) in all composite flexible films, calculated via infrared spectroscopy and differential scanning calorimetry (DSC).

Table 2. Comparison of dielectric pemittivity an dielectric loss tangent (at RT and f = 1 kHz) obtained in this work with those reported in the literature on other lead-free ferroelectric ceramics/PVDF flexible composites.

Table 3. The density, measured with Archimedes's method, the fundamental resonance frequency at room temperature and the corresponding Young's modulus of the three compositions.

Table 4. Electric displacement, maximum electric field, dielectric permittivity values at 1 kHz, energy storage density and energy density efficiency for composites and neat PVDF film.

Figure 1

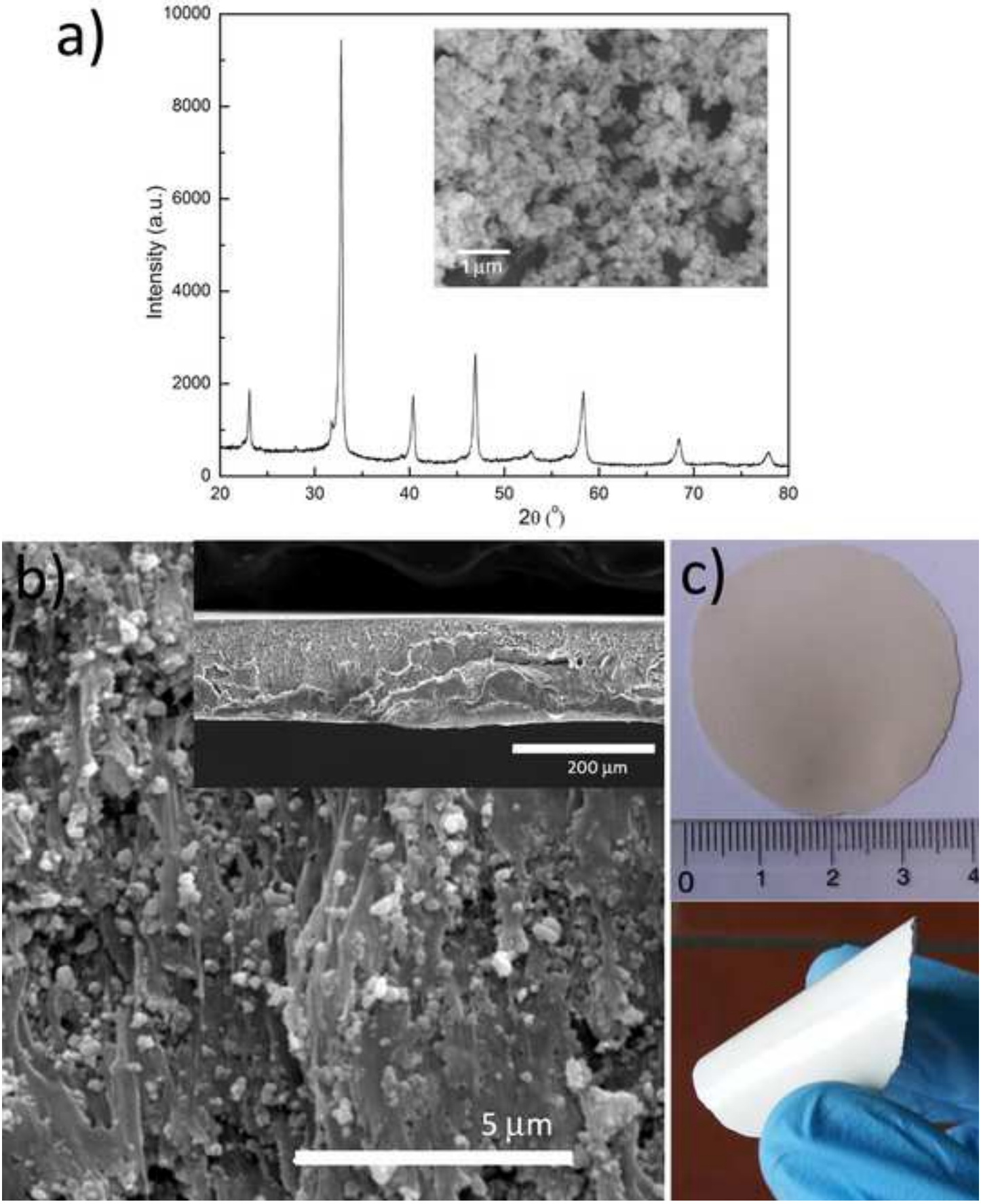

Figure 2

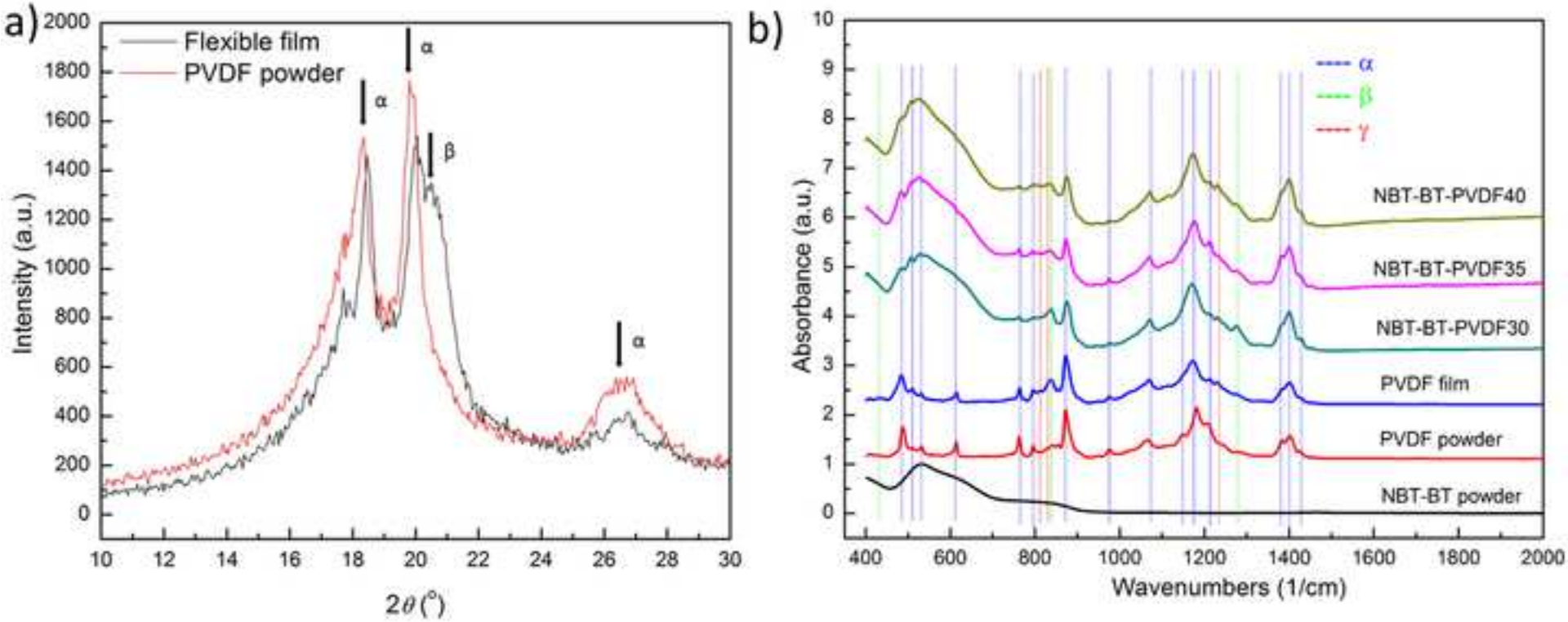

Figure 3

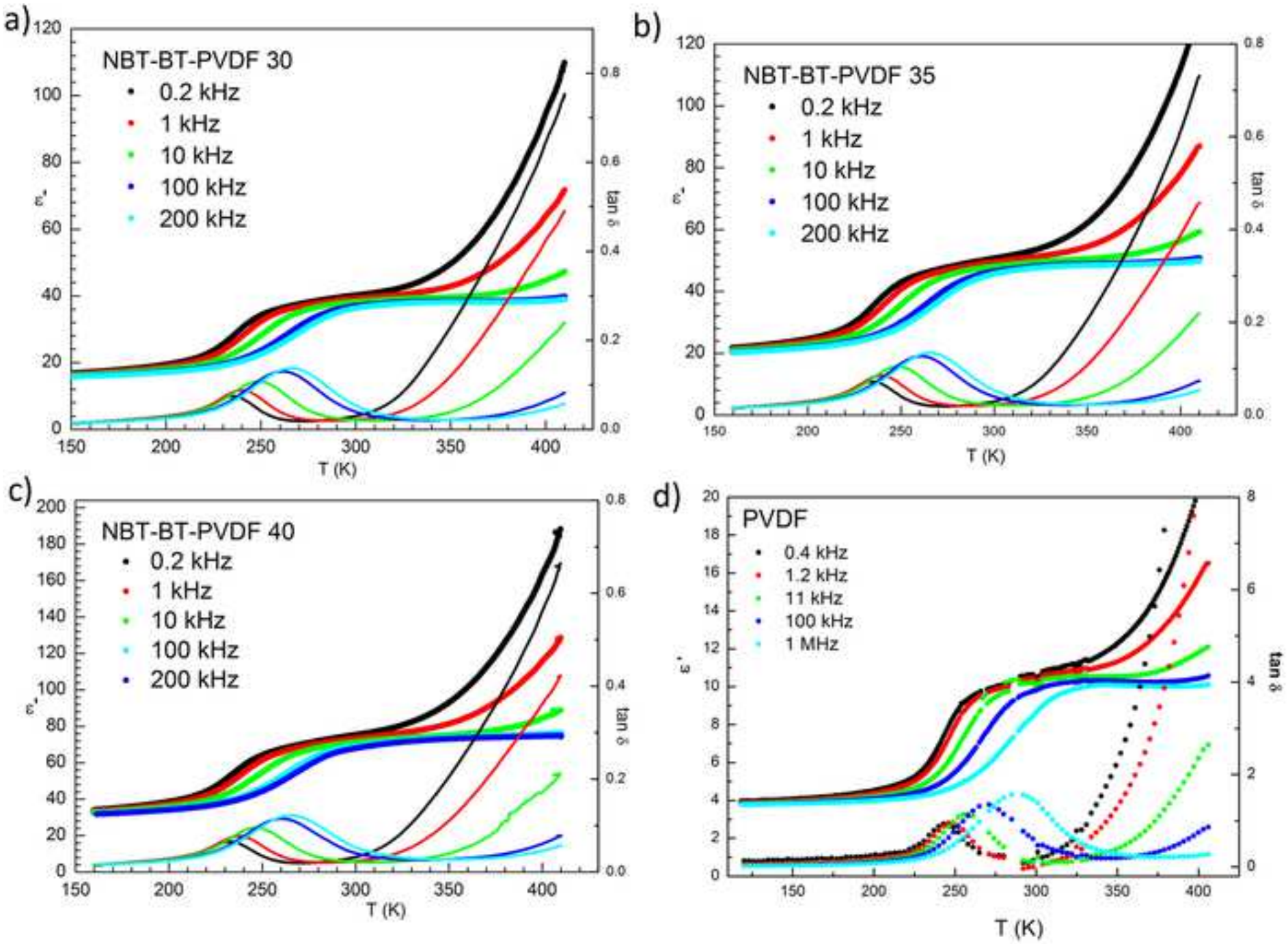

Figure 4

Click here to access/download;Figure;Figure 4.tif

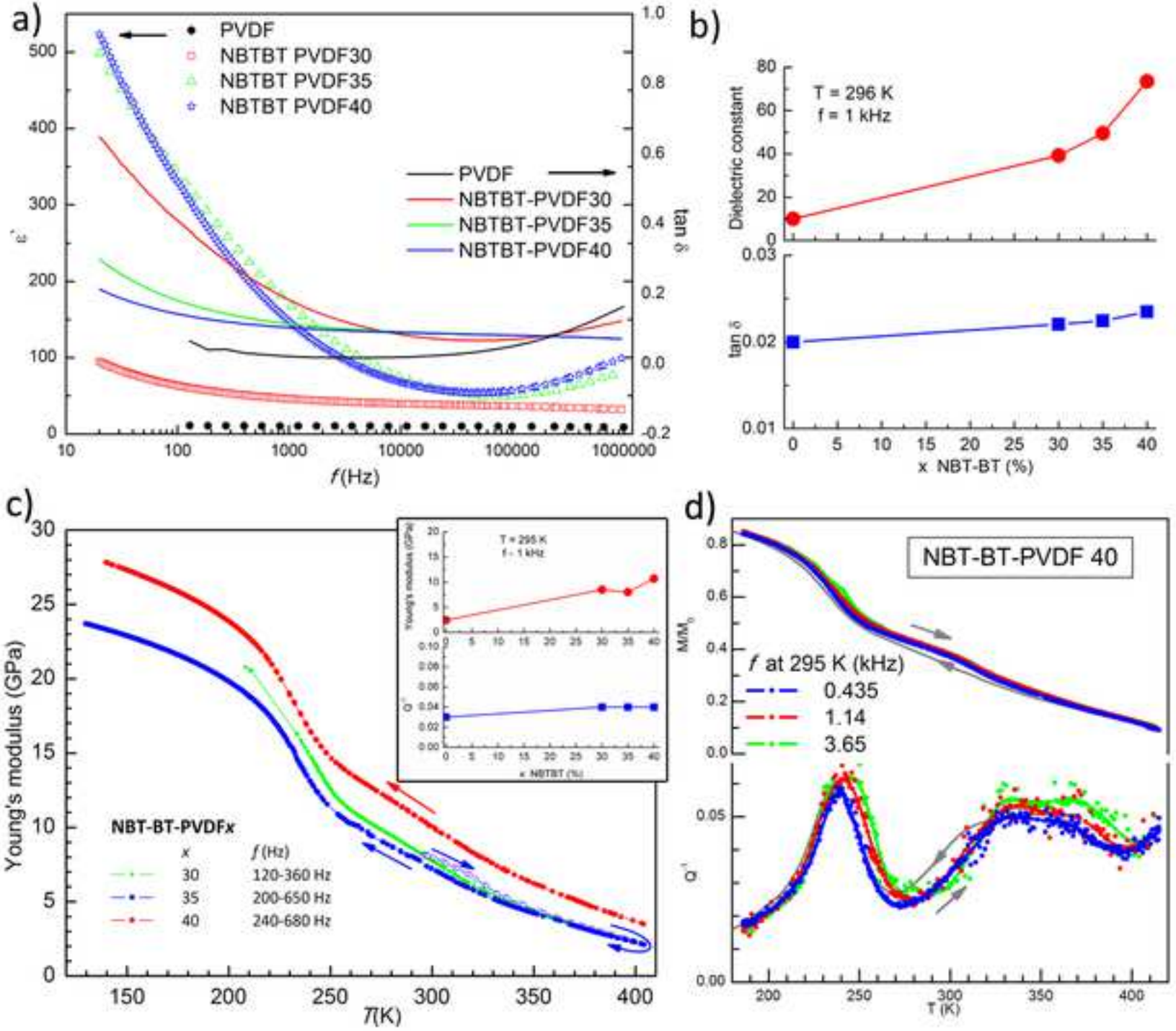

Figure 5

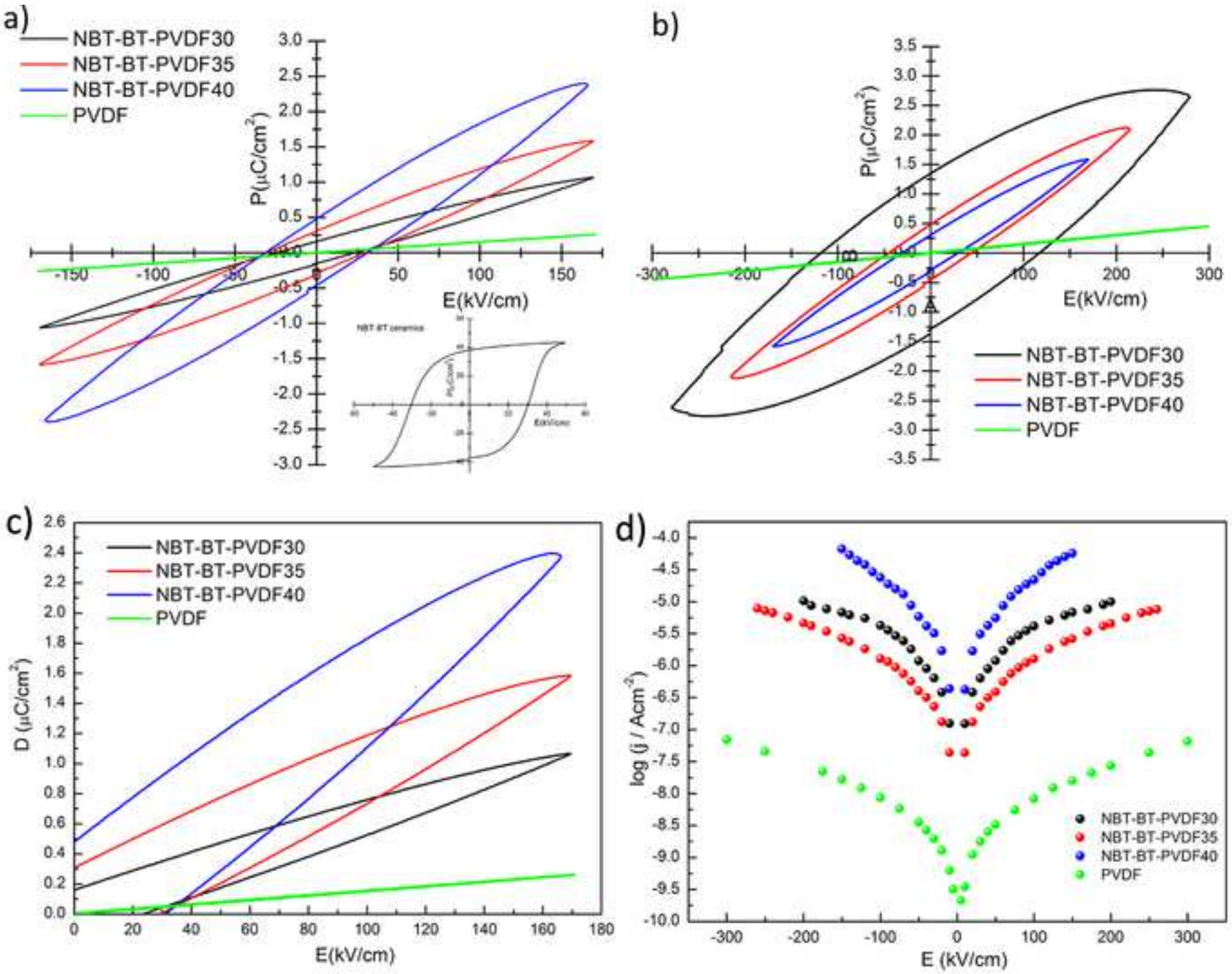

Figure 6a and b

Click here to access/download;Figure;Fig. 6a and b.tif

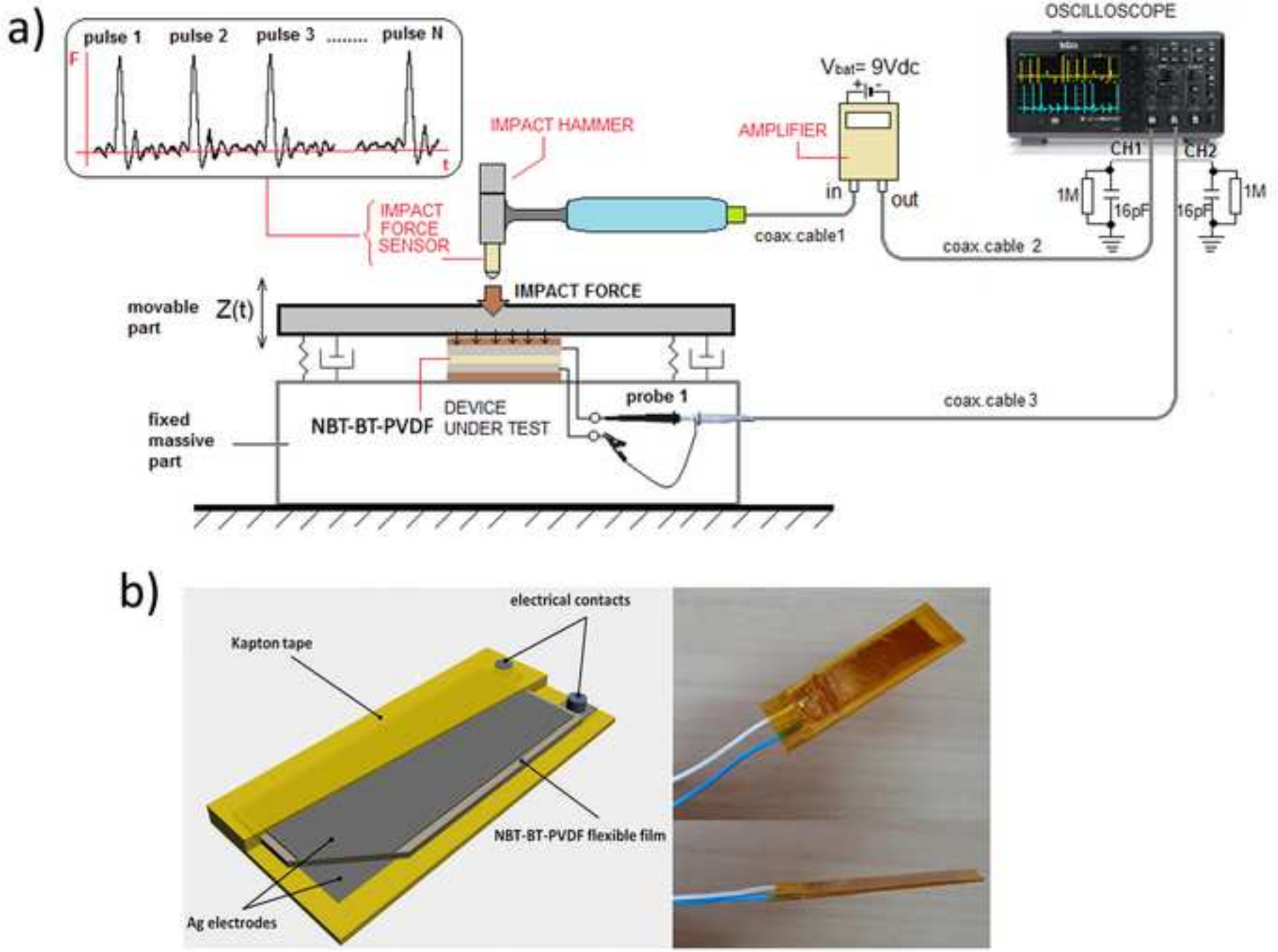

Figure 6c

Click here to access/download;Figure;Fig. 6c.tif

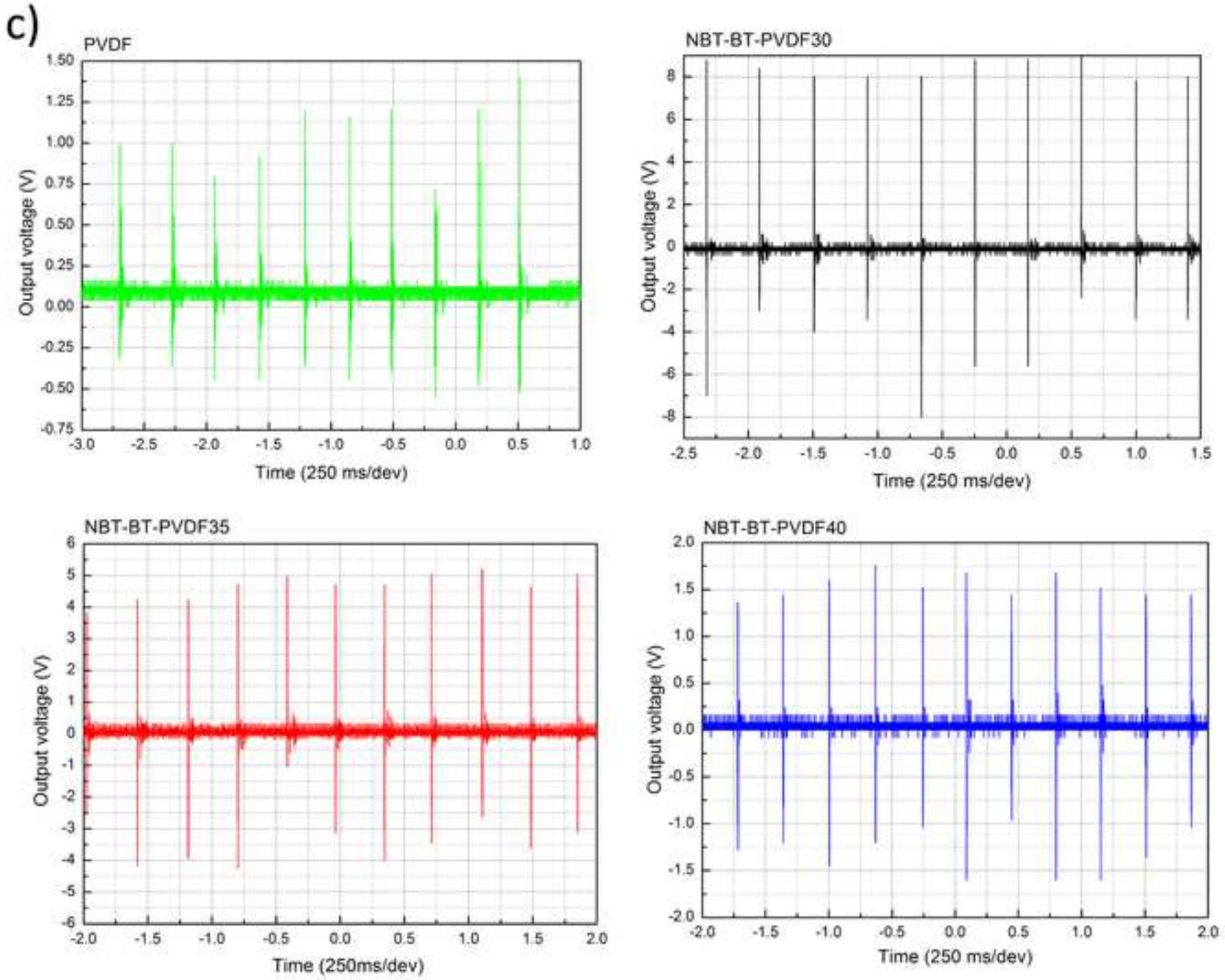

Figure captions

Figure 1. a) XRD and inset SEM of NBT-BT powder, calcined at 800°C x 1h, used for flexible films preparation, b) SEM representing surface of the film, inset SEM of the transversal internal surface of the film c) Flexible film NBTBT-PVDF35

Figure 2. a) XRD pattern for PVDF powder and neat PVDF film, b) FT-IR spectrum of powders and flexible films

Figure 3. a) Dielectric permittivity and dielectric losses vs. temperature for NBT-BT-PVDF flexible films for different compositions and frequencies, as specified on the graphs

Figure 4. a) Dielectric permittivity and dielectric loss tangent vs. frequency for all flexible samples, b) Variation of dielectric permittivity and loss, measured at ambient temperature and 1 kHz, with the content of NBT-BT phase in the composite flexible films, c) Young's modulus measured exciting the 1st flexural mode of NBT-BT-PVDF30, 35 and 40 composite samples during cooling; the initial heating is also shown for the 35% sample (empty symbols), as an inset Young's modulus and elastic energy loss at 295 K vs. composition, d) Relative change of the Young's modulus and elastic energy loss vs. *T* of NBT-BT-PVDF40 measured alternately exciting three flexural resonances during a same heating run

Figure 5. Ferroelectric properties of neat PVDF and all composite films at a) 170 kV/cm and as an inset hysteresis loop of NBT-BT ceramics, b) at the highest reached field for each sample, c) Displacement vs. electric field loops and d) leakage current density vs. electric field for neat PVDF and all composite flexible films

Figure 6. a) Scheme of testing set-up and b) Scheme of the energy harvesting and storage component and picture of the assembled one, c) Oscilloscopic records of the voltage output obtained by applying the impact force